



Generation and Enrichment of Pedestrian Maps with Vertical Shadows in Urban Environments from Mobile Laser Scanning Data

Jesús Balado^{*1,2}, Lucía Díaz-Vilariño¹, Ernesto Frías¹, Elena González¹

¹Universidad de Vigo, CINTECX, GeoTECH group. 36310 Vigo, España (jbalado, lucia, efrias, elena)@uvigo.es

²Delft University of Technology, Faculty of Architecture and the Built Environment, GIS Technology Section. 2628 BL Delft, The Netherlands (J.BaladoFrias@tudelft.nl)

*Correspondence: J.BaladoFrias@tudelft.nl

Abstract

Cities are becoming more pedestrian-friendly, reducing traffic and promoting physical activity and walking. However, prolonged exposure to the sun can cause sunburn and skin problems, so minimizing exposure to the sun while travelling is especially relevant at certain latitudes and in the summer months. This paper proposes a method for modelling urban contours and generating pedestrian maps with the location of shaded areas and accessibility barriers. The proposed method uses as input data a point cloud of an urban environment acquired with Mobile Laser Scanning. First, the input point cloud is segmented in ground points, obstacle points, and points causing shadows. Then, the three segmented point clouds are rasterized and the corresponded images are combined to obtain the navigable ground and the shaded areas. Finally, from the navigable ground, a navigation map is generated for pedestrians. To check the usefulness of this navigation map, a pathfinding algorithm is applied. The results show a correct generation of the navigable ground, and routes prioritizing the trajectory by shadow areas. Depending on the weighting between sun and shaded areas, the routes obtained show differences in distance travelled and sun exposure. The proposed method is sensitive to the existence of obstacles and noise in the point clouds.

Keywords: point clouds, physical accessibility, people with disabilities, wheelchair, navigation, sun exposure

Received: September 11th, 2020/ Accepted: December 2nd, 2020 / Online: December 12th, 2020

I. INTRODUCTION

The increase in population in cities is causing difficulties in the space available for vehicles (traffic jams and parking lots) as well as problems for the health of the inhabitants (increase in the levels of pollution and noise). For these reasons, cities are being redesigned, shifting from a car-centered model to a pedestrian-centered model [1]. The pedestrian-centered model requires more friendly infrastructures for short walking trips combined with a public transport network that facilitates large travel and smooth access to the city.

The shift to pedestrian-centered cities is performed first administratively and then constructively, so old infrastructures get new pedestrian uses for which they were not designed [2]. Often the changeover happens abruptly and at specific times. In certain events, squares and streets can be closed to traffic to allow more people or more physical distance between them.

The navigation of pedestrians in complex urban environments is influenced by several factors. One of the most

influencing factors is the physical accessibility [3] which, although it is not a problem for people without reduced mobility, curbs and steps considerably hinder the movement of people in wheelchairs. Another key factor is exposure to solar radiation. Many events are organized exclusively in summer season. Excessive UV radiation can cause an immediate effect of sunburn [4] and serious long-term illnesses [5]. As a result, in sectors such as tourism, sun-protective behaviors are being promoted [6].

Point clouds have proven to be a very useful source of geometric data for analyzing urban ground and physical accessibility. Curbs or stairs have associated a semantic characteristic of accessibility. In point clouds, steps can be identified by means of geometry and/or topology [7–9]. Steps and ramps are also detectable at building entrances point clouds, obtaining the accessibility information of the associated service [10]. By changing the perspective, physical accessibility can be analyzed based on the movement of the human body according to their dimensions [11] or degrees of freedom [12,13]. In

addition, some authors have used Mobile Laser Scanning (MLS) point clouds to generate maps according to different mobility profiles in urban environments with squares and streets at different altitude levels and numerous pedestrian crossings [14,15]. Likewise, Aerial Laser Scanning (ALS) point clouds acquired allow the calculation of the solar incidence on roofs, in order to increase energy production of solar panels or detect roofs hidden by higher buildings [16].

The aim of this work is to generate specific maps for pedestrians (distinguishing people without reduced mobility and wheelchair users) from MLS point clouds, detecting and prioritizing shadow areas produced by objects and buildings in the urban environment. In this work only pedestrian areas are analyzed, so it is not necessary to segment urban ground elements, because citizens can navigate freely through squares and areas closed to traffic, although people in wheelchairs are limited in their mobility because of steps. Nor is it necessary to differentiate the classes of objects, a topic extensively studied [17–19], since this works focuses on the shadow they produce.

This paper is structured as follows. In section 2, the designed method is explained. In section 3, the case studies, and the results of the application of the method are presented. Section 4 is dedicated to the discussion and section 5 concludes this paper.

II. METHOD

The designed method uses an MLS point cloud of an urban environment as input data. All land is assumed as safe and available for pedestrian navigation in the input data. The method consists of three main processes. First, the point cloud is

Second, the navigable and shadowed ground is obtained from rasterization and superimposition of the segmented point clouds. And third, the map is generated for navigation. Fig. 1 shows the detailed workflow of the work.

A. Segmentation

There are three relevant elements for navigation with shadows knowledge: the ground, since it is the surface where the pedestrian navigates and which is going to be modelled; the obstacles that delimit the navigable ground; and the objects that generate shadows on the ground. In order to differentiate these elements, the segmentation is based on the delimitation of a region of interest (ROI) and the calculation of the tilt of each point. The ROI is defined by detecting the ground plane and a maximum height corresponding to $h = 2$ m, which is the height required for a pedestrian walks comfortably according to the ISO 21.542 [20]. Outside the ROI are located the points that can produce shadows and inside the ROI are located the ground points and obstacles to navigation.

The ground plane detection plane is performed with M-estimator SAMple Consensus (MSAC) [21]. The ground is assumed as a horizontal plane that may have small variations in steps or punctual inclination changes. But also, the urban ground can be a completely sloping surface, although this slope is limited to keep a navigable surface. The detection of the ground plane with MSAC focuses on the search of points grouped in a horizontal surface defined by the direction of the normal to the ground (0.0.1) and admitting a maximum variation in the inclination up to 20° . Using the detected ground plane as base, a 3D polygon of height h is generated. The interior of the polygon is the ROI where the navigable ground and obstacles are found. The points outside of the ROI, those points with a height greater than h , are considered as shadowing points (Fig. 2).

Within the ROI, the surface normals $N(N_x, N_y, N_z)$ of the points are estimated with respect to their nearest 25 neighbors [22] to differentiate between points belonging to navigable ground and objects. Normals are used to calculate the tilt of each point (1). Then, points are classified by their inclination in horizontal ($tilt < 20^\circ$) and vertical ($tilt > 20^\circ$). A surface with an inclination of less than 20° allows a comfortable movement for a pedestrian. Horizontal points correspond largely to the ground and vertical points to obstacles. Although some points are

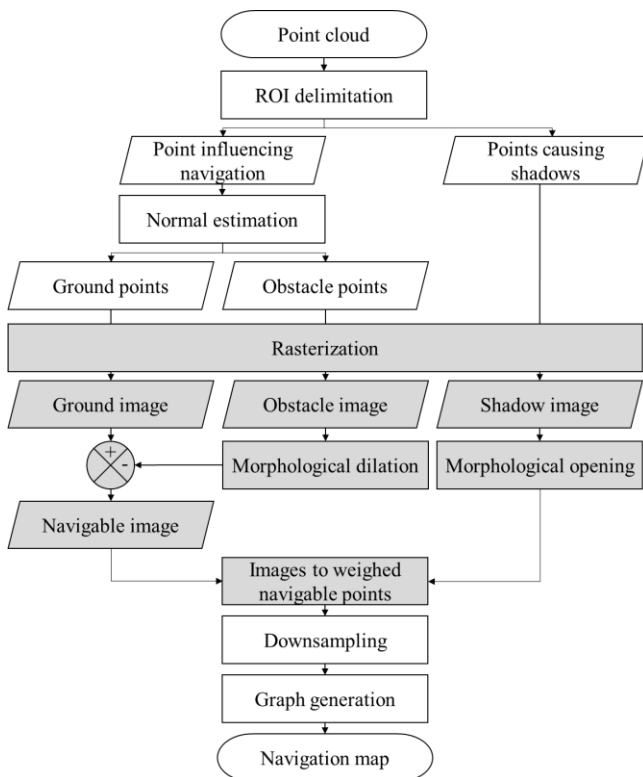


Fig. 1. Workflow of the proposed method

segmented into ground points, obstacles, and shadowing objects.

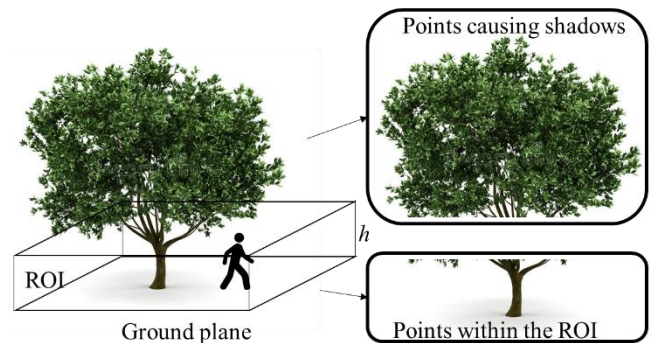


Fig. 2. Delimitation of the Region of Interest

erroneously classified as ground because not all horizontal points are ground, these points are removed in the next section.

$$\text{tilt} = \tan^{-1} \frac{\sqrt{N_x^2 + N_y^2}}{N_z} \quad (1)$$

B. Navigable and shadowed ground estimation

The navigable ground is the ground suitable for pedestrian traffic. In order to know which part of the ground corresponds to navigable ground and also which part is in shadow areas, the previously segmented point clouds are projected on Z axis by means of a rasterization (Fig. 3) with a size of pixel r [23]. Then, the generated raster images are overlapped.

From the segmented ground points, the ground image is obtained. Any pixel containing a horizontal point is ground pixel in the raster image. The ground raster image serves as the basis for the subsequent generation of the navigation map.

The segmented obstacle points generate two different obstacle images according to the pedestrian motor skills: person without reduce mobility and person in a wheelchair. The obstacle images are generated from the difference in height of the points belonging to each pixel. In the case of persons without reduced mobility, if the difference in height is greater than 15 cm (maximum step height defined by ISO 21.542), it is considered as obstacle pixel. In the case of wheelchairs, obstacle pixels are those with a difference in height greater than 5 cm.

Obstacles influence the navigable ground according to the free unobstructed space they leave behind. The minimum free unobstructed space in width w is obtained from the ISO 21.542. The minimum width for pedestrians is 0.8 m and for wheelchairs is 1.0 m. Therefore, the obstacles raster image is expanded to a pixel size according to $w/2$ pixels with a circle-shaped structuring element. The dilated obstacle pixels are subtracted from the ground pixels. In this way, ground pixels which are too close to objects are discarded as navigable ground. This also includes ground pixels generated by horizontal points erroneously considered as ground in the previous subsection.

The points causing shadows generate the shadow raster image. A shadow pixel contains shadowing points. However, the upper areas of the point cloud often contain noise and objects too small to generate useful shadows for pedestrians. A morphological opening is applied to shadow raster image with a 3x3 pixel square-shape structuring element to filter small shadows. A completely vertical projection of the shadows has been assumed, which corresponds approximately to the central hours of the day and when the sun's rays are most intense. The ground pixels that match the shadow pixels are assigned a shadow label.

To complete the process of calculating navigable and shadowed ground, the navigable ground raster image with shadow information is transformed to a point cloud. For the points belonging to each navigable ground pixel, the midpoint is calculated. An attribute with value 1 is assigned if the pixel corresponds to a non-shadowed area, and value p if the navigable ground pixel corresponds to a shadow.

C. Graph generation

At the end of the generation of the navigable ground, a point cloud distributed on a 2D grid with a Z component and a shadow attribute is obtained. The distance between consecutive points is defined by the grid pixel size r with small variations in the Z component.

For pedestrian navigation, a node density as high as the grid size is not required, so the density is reduced to obtain a minimum distance of $d = 0.5$ m between consecutive points. Since shadow and non-shadow points can coincide in the same simplified point, the attribute p of the new point is averaged from p of simplified points.

The navigation map proposed for this work is a dense map, with points distributed regularly as in a cellular automata [24], but organized by means of nodes and arcs as in a conventional navigation map. For the generation of the network that corresponds to the navigation map, the nodes correspond to the downsampled points. The arcs are calculated from the neighborhoods with D8 connectivity between points, which allows to obtain routes in orthogonal and diagonal. The equivalent of the D8 connectivity search in the grid-structured point cloud is done by searching for points at a distance less than $\sqrt{2}d$. Finally, the distance of the arcs is weighted and calculated as $l_p = l \cdot p$, where l is the 3D Cartesian distance between the points.

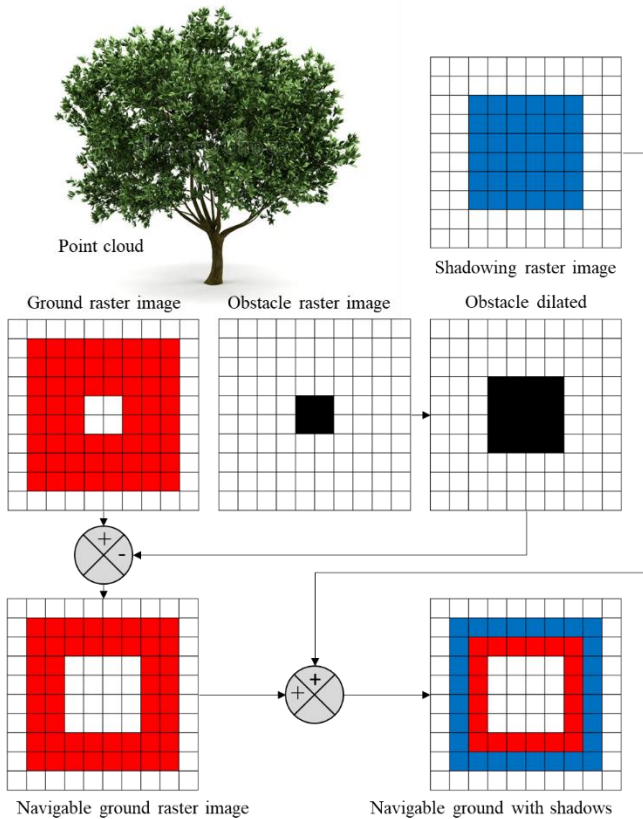


Fig. 3. Raster image overlapping process for the generation of navigable shadow ground

III. EXPERIMENTS

A. Datasets and equipment

The designed method was tested in two real case studies. The first one corresponds to the *Praça da Liberdade* in Porto (Portugal). The square is delimited on its four sides by roads with regular traffic, separated from the sidewalks by curbs. The center of the square is empty, except for an equestrian statue. On the edges of the sidewalks there are trees, street lights, traffic signs and various street furniture, as well as bar terrace areas. The place is often used as a concert zone, visualization of football matches and other events, besides being an area of great tourist confluence. The second case study corresponds to the *Praza do Concello* in *Salceda de Caselas* (Spain). It is a square of reduced dimensions and closed to the traffic permanently. In the square there are mixed wooded areas, with open spaces and diverse furniture, among which are benches. The area is used weekly for the celebration of the market and outdoor activities. In both case studies, maximum temperatures of 35° are exceeded in the summer months.

The point clouds of the case studies (Fig. 4) contain 24.1 million points and 13.4 million points, respectively. Although the point density presents strong variations depending on the distance to the MLS trajectory acquisition, the average ground point density is 800 points/m² in case study 1 and 1400 points/m² in case study 2. They were acquired with LYNX Mobile Mapper of Optech [25]. The algorithm was implemented in Matlab and processed on an CPU i7-7700HQ 2.8Ghz with 16GB RAM DDR4. The processing time to obtain the navigation maps was 220 s and 240 s for the first dataset and 75 s for the second.

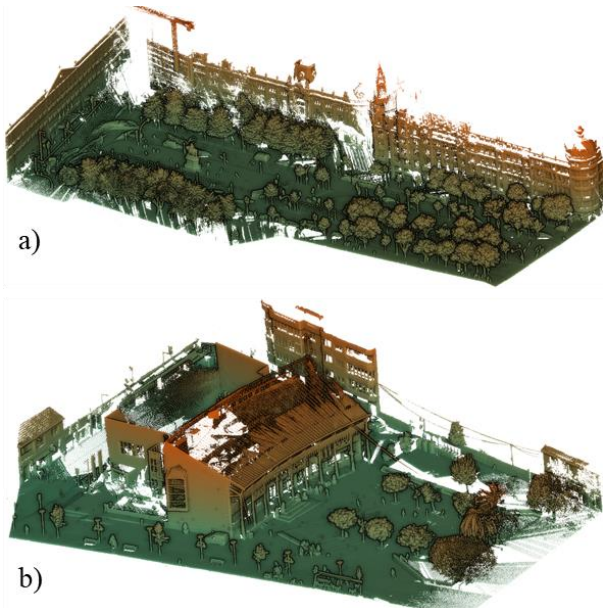


Fig. 4. Point clouds of: a) *Praça da Liberdade* in Porto and b) *Praza do Concello* in *Salceda de Caselas*. Note: The front façade line was removed to improve de visualization

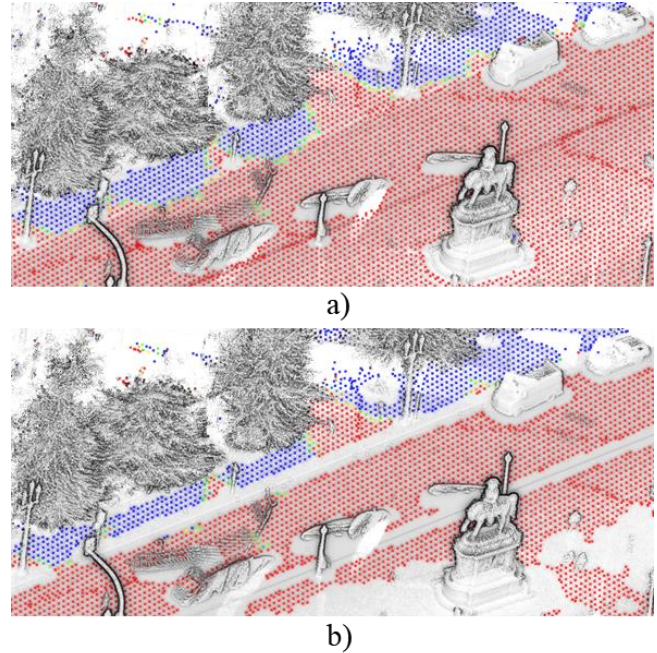


Fig. 5. Map of navigable nodes for people without reduced mobility (a) and people in wheelchairs (b) from the case study 1. Color gradient of sunny areas (red), semi-shadow (yellow and green) and shadow (blue)

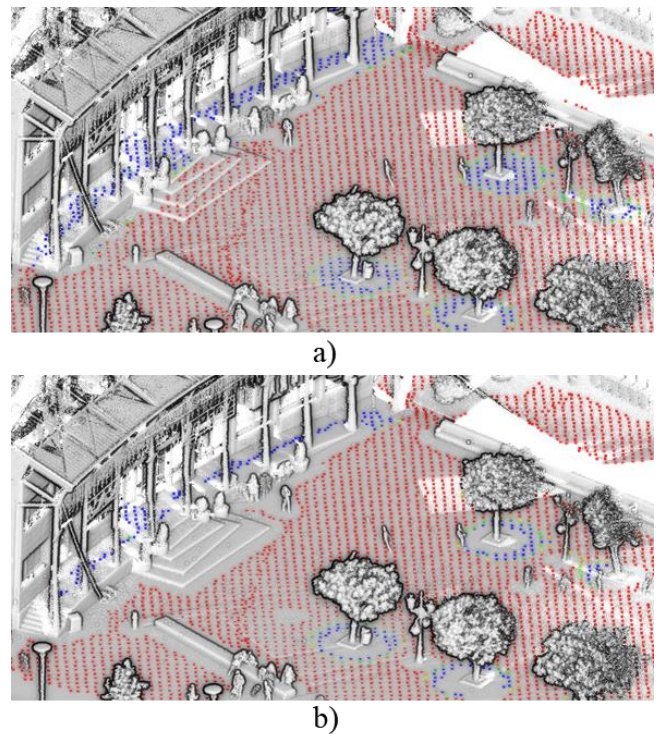


Fig. 6. Map of navigable nodes for people without reduced mobility (a) and people in wheelchairs (b) from the case study 2. Color gradient of sunny areas (red), semi-shadow (yellow and green) and shadow (blue)

B. Results of navigable shadow ground

The grid size of the raster has been experimentally set at $r = 0.2$ m. This size was the minimum that ensured a correct detection of steps from the height difference in the points of each pixel.

Fig. 5 and Fig. 6 show the navigable points acting as nodes in the navigation map. The nodes are separated by an average distance of 0.5 m from their four nearest orthogonal nodes. A regular distribution of the nodes can be observed. The blue points denote shadows, areas under another surface, either tree or building. Between the sunlight (red) and shaded (blue) points, a small transition gradient (yellow-green) can also be observed in the colored points.

There were two main differences between the nodes for people without reduced mobility and people in wheelchairs. The largest is the absence of navigable nodes on steps and curbs on wheelchair maps. The second is the reduction in the size of the navigable surface also on wheelchair maps since the necessary free unobstructed space is greater for wheelchairs than for people without reduced mobility.

C. Results of pathfinding

The Dijkstra's algorithm was selected for the pathfinding application on navigation map. Dijkstra's algorithm has been chosen for its robustness and has been tested in many applications [26]. The value p for the following tests has been set to 0.5 and each route was calculated in less than 0.01 s on the computer above-mentioned. Fig. 7 shows two routes calculated in the case study 1 with the same start and end point. Both trajectories prioritized the shaded areas and minimize the sun exposure. The route in Fig. 7.a corresponded to a route for people without reduced mobility. The route crossed a curb. The route in Fig. 7.b is a route for a person in wheelchair. The route was conditional on crossing a ramp due to curbs are no navigable for wheelchairs. The route for pedestrians was straighter and had less exposure to the sun.

The pathfinding algorithm was also applied in the navigation map of case study 2. The route in Fig. 8.a was a route for people without reduced mobility. It took advantage of the building portico to cover half of the trajectory in the shadow area. The route crossed two sections of steps. In the Fig. 8.b, the trajectory varied to fit in with the tree shadow area, when it headed to the access ramp, as it was a route for wheelchairs.

D. Discussion

The proposed method and navigation maps showed logical results in the estimation of navigable routes, both for people without reduced mobility or in wheelchairs, always prioritizing the shadow areas. The value p of the shadow weighting was very subjective, and it was dependent to each user to establish what weight is assigned to avoid sunny areas. Fig. 9 shows the comparison of four different weightings in value p . With $p = 1$, which is equivalent to no weighting, the route was as straight as possible based on navigable ground. As the value p was decreased, the shaded areas were prioritized, and the size of the route were increased. With a $p = 0.25$, the route was completely

prioritized by the shadow until it reached the shaded node nearest the destination and then, it crossed in a straight line to the end node. Although all routes with different p values were correct, the choice of p varied the total distance travelled. With the choice of p , the user can select the desired route in the balance of sun exposure and distance travelled.

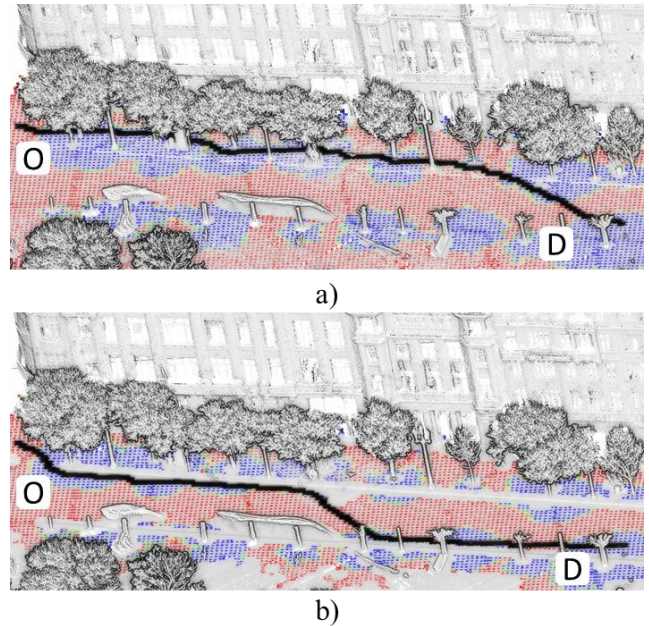


Fig. 7. Routes (in black) calculated in case study 1 for people without reduced mobility (a) and in a wheelchair(b) maximizing the shaded areas. Note: Origin marked with O and destination with D.

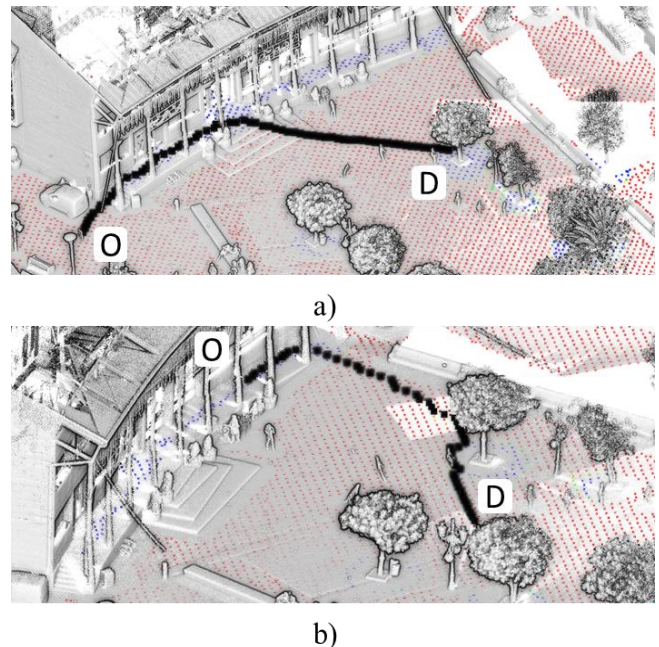


Fig. 8. Routes (in black) calculated in case study 2 for people without reduced mobility (a) and in a wheelchair(b) maximizing the shaded areas. Note: Origin marked with O and destination with D.

The correct route calculation depends on the navigable ground modelled with the proposed method. The algorithm was not free of undesired behaviors derived from the MLS acquisition and input point clouds. The point clouds were acquired without cutting off road or pedestrian traffic. For this reason, these dynamic objects (which can be observed in the figures) were considered as obstacles in the generation of a navigable map and therefore the obstacles avoided nodes in the navigation maps. In addition, both dynamic and static objects also generate occlusions in the ground and produce gaps in the navigable ground (Fig. 10.b). Another problem that appeared was caused by noise. The calculation of steps was particularly sensitive to the noise. In Fig. 10.a, the area around the statue does not have any steps but the algorithm considered it as a non-navigable area for wheelchair users. Expanding this area (Fig. 10.c), three parallel ground planes were located with different densities, spaced at 0.08 m and 0.03 m. These distances were greater than the height considered as comfortably salvageable by a wheelchair, and therefore that area was considered as non-navigable by the algorithm for wheelchair users.

The proposed method is based on a series of parameters, whose values are justified based on ISO 21.542. The free unobstructed space set in this work (and differentiated in height and width) may not be sufficient for many people. Modification of these parameters based on the physical characteristics of each person would provide personalized mobility maps. As far as the urban environment is concerned, although the case

studies correspond to areas with low inclination, there are urban areas which, because of their location, have ground with inclinations greater than 20 degrees complicate the movement of all pedestrians. In these cases, it should be assessed whether to consider high-inclined ground as non-navigable, with the consequent loss of nodes and limitation in pathfinding, or to maintain them by modifying the maximum tilt.

Finally, in this work the shadow zone was established as the vertical zones, this simplification is common to all urban areas of the world. However, as a future work, the detection of the shadow zones according to the inclination of the sun is contemplated, which will vary the shadow zones according to the time of day, the day of the year and the geographical location of the urban area.

IV. CONCLUSION

In this work, a method for modelling urban environments and obtaining pedestrian navigation maps with shadow areas and physical accessibility information data has been presented. The method is based on the detection of navigable ground by two motor skills (people without reduced mobility and people in wheelchairs) and the detection of the shadowing points. This information is overlapped by a raster process and a navigation map is generated. Then, the pathfinding Dijkstra's algorithm is applied. The generated routes prioritize the shadow areas and minimize the sun exposure according to a p weighting variable with the aim of obtain a balance defined by the end user between distance traveled and sun exposure. The routes are also fully accessible according to the selected motor profile. In addition, the maps are generated in minutes and the routes are calculated in real time. In view of the results, MLS point clouds are a very useful source of data for the generation of pedestrian maps that integrate accessibility features and shadow zones. Likewise, the generation of maps from precise 3D data of the environment makes it possible to obtain customizable maps according to the physical and motor skills of each citizen.

As a future work, an oblique projection of the shadows will be implemented, given the Z component of the shadowing points and the trajectory of the sun are known, while this work was limited to a vertical shadow projection. Noise minimization in input point clouds and its effect on step detection will also be studied.

ACKNOWLEDGMENT

Authors would like to thank to the Xunta de Galicia given through human resources grant (ED481B-2019-061, ED481D 2019/020), that has made possible the collaboration with TUDelft, and competitive reference groups (ED431C 2016-038), the Ministerio de Ciencia, Innovación y Universidades - Gobierno de España- (RTI2018-095893-B-C21, PID2019-105221RB-C43). This project has received funding from the European Union's Horizon 2020 research and innovation programme under grant agreement No 769255. This document reflects only the views of the author(s). Neither the Innovation and Networks Executive Agency (INEA) or the European Commission is in any way responsible for any use that may be made of the information it contains. The statements made herein are solely the responsibility of the authors.

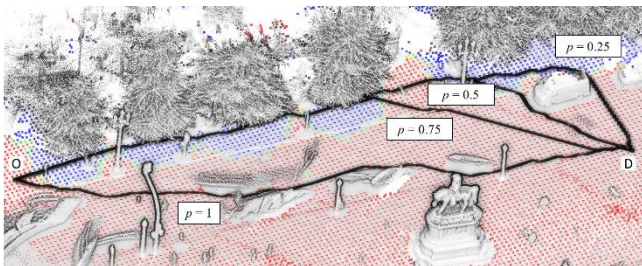


Fig. 9. Differences in the calculation of routes according to variation of value p in a navigation map for people without reduced mobility. Note: Origin marked with O and destination with D.

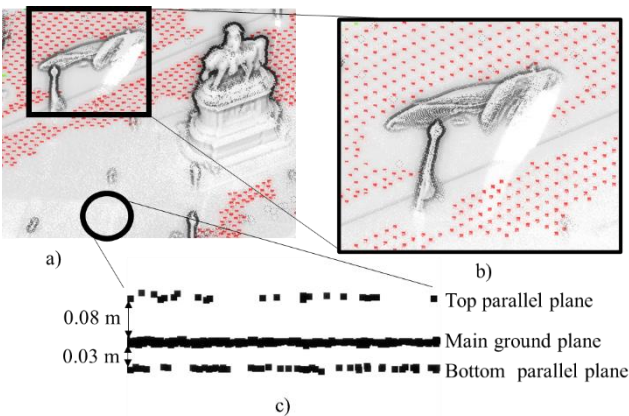


Fig. 10. Limitations in the proposed method: a) Point cloud of case study 1 with enlarged navigation map for wheelchairs, b) gaps in the navigation map generated by circulating cars, c) parallel ground acquired with an inaccurate registration

REFERENCES

- [1] U. Kozan, S.S. Uzunoglu, The Importance of Pedestrianization in Cities-Assessment of Pedestrianized Streets in Nicosia Walled City, *European Journal of Sustainable Development*. 9 (2020) 589. <https://doi.org/10.14207/ejsd.2020.v9n2p589>.
- [2] K. Pogačar, P. Senk, Alternative approaches and tools for the transformation of streetscapes: Direct physical interventions and different modes of participation, *Prostor*. 26 (2018).
- [3] R.L. Church, J.R. Marston, Measuring Accessibility for People with a Disability, *Geographical Analysis*. 35 (2003) 83–96. <https://doi.org/10.1111/j.1538-4632.2003.tb01102.x>.
- [4] A. Zamanian, C. Hardiman, Electromagnetic radiation and human health: A review of sources and effects, *High Frequency Electronics*. 4 (2005) 16–26.
- [5] S.N. Byrne, How much sunlight is enough?, *Photochemical & Photobiological Sciences*. 13 (2014) 840–852.
- [6] A. Rodrigues, F.F. Sniehotta, V. Araujo-Soares, Are Interventions to Promote Sun-Protective Behaviors in Recreational and Tourist Settings Effective? A Systematic Review with Meta-analysis and Moderator Analysis, *Annals of Behavioral Medicine*. 45 (2012) 224–238. <https://doi.org/10.1007/s12160-012-9444-8>.
- [7] A. Serna, B. Marcotegui, Urban accessibility diagnosis from mobile laser scanning data, *ISPRS Journal of Photogrammetry and Remote Sensing*. 84 (2013) 23–32. <https://doi.org/10.1016/j.isprsjprs.2013.07.001>.
- [8] J. Balado, L. Díaz-Vilariño, P. Arias, H. González-Jorge, Automatic classification of urban ground elements from mobile laser scanning data, *Automation in Construction*. 86 (2018) 226–239. <https://doi.org/10.1016/j.autcon.2017.09.004>.
- [9] K. Ishikawa, D. Kubo, Y. Amano, Curb Detection and Accessibility Evaluation from Low-Density Mobile Mapping Point Cloud Data, *International Journal of Automation Technology*. 12 (2018) 376–385.
- [10] J. Balado, L. Díaz-Vilariño, P. Arias, I. Garrido, Point Clouds To Indoor / Outdoor Accessibility Diagnosis, *ISPRS Annals of the Photogrammetry, Remote Sensing and Spatial Information Sciences; ISPRS Geospatial Week 2017. IV-2/W4* (2017) 18–22. <https://doi.org/doi.org/10.5194/isprs-annals-IV-2-W4-287-2017>.
- [11] L. Díaz-Vilariño, P. Boguslawski, K. Khoshelham, H. Lorenzo, L. Mahdjoubi, Indoor navigation from point clouds: 3D modelling and obstacle detection, *The International Archives of the Photogrammetry, Remote Sensing and Spatial Information Sciences*. XLI-B4 (2016) 275–281. <https://doi.org/10.5194/isprsarchives-XLI-B4-275-2016>.
- [12] T. Maruyama, S. Kanai, H. Date, M. Tada, Simulation-Based Evaluation of Ease of Wayfinding Using Digital Human and As-Is Environment Models, *ISPRS International Journal of Geo-Information*. 6 (2017). <https://doi.org/10.3390/ijgi6090267>.
- [13] T. Maruyama, S. Kanai, H. Date, M. Tada, Motion-capture-based walking simulation of digital human adapted to laser-scanned 3D as-is environments for accessibility evaluation, *Journal of Computational Design and Engineering*. 3 (2016) 250–265. <https://doi.org/https://doi.org/10.1016/j.jcde.2016.03.001>.
- [14] G. López-Pazos, J. Balado, L. Díaz-Vilariño, P. Arias, M. Scaioni, Pedestrian pathfinding in urban environments: Preliminary results, in: *ISPRS Annals of the Photogrammetry, Remote Sensing and Spatial Information Sciences*, Kyiv, Ukraine, 2017: pp. 4–6. <https://doi.org/doi.org/10.5194/isprs-annals-IV-5-W1-35-2017>.
- [15] J. Balado, L. Díaz-Vilariño, P. Arias, H. Lorenzo, Point clouds for direct pedestrian pathfinding in urban environments, *ISPRS Journal of Photogrammetry and Remote Sensing*. 148 (2019) 184–196. <https://doi.org/10.1016/j.isprsjprs.2019.01.004>.
- [16] M. Soilán, B. Riveiro, P. Liñares, M. Padín-Beltrán, Automatic Parametrization and Shadow Analysis of Roofs in Urban Areas from ALS Point Clouds with Solar Energy Purposes, *ISPRS International Journal of Geo-Information*. 7 (2018). <https://doi.org/10.3390/ijgi7080301>.
- [17] Y. Ye, H. Chen, C. Zhang, X. Hao, Z. Zhang, SARPNET: Shape attention regional proposal network for LiDAR-based 3D object detection, *Neurocomputing*. 379 (2020) 53–63. <https://doi.org/https://doi.org/10.1016/j.neucom.2019.09.086>.
- [18] M. Engelcke, D. Rao, D.Z. Wang, C.H. Tong, I. Posner, Vote3Deep: Fast object detection in 3D point clouds using efficient convolutional neural networks, in: *2017 IEEE International Conference on Robotics and Automation (ICRA)*, 2017: pp. 1355–1361. <https://doi.org/10.1109/ICRA.2017.7989161>.
- [19] G. Pang, U. Neumann, 3D point cloud object detection with multi-view convolutional neural network, in: *2016 23rd International Conference on Pattern Recognition (ICPR)*, 2016: pp. 585–590. <https://doi.org/10.1109/ICPR.2016.7899697>.
- [20] ISO, ISO-21542 Building construction — Accessibility and usability of the built environment, *ISO International Organization for Standardization*. (2011).
- [21] P.H.S. Torr, A. Zisserman, MLESAC: A New Robust Estimator with Application to Estimating Image Geometry, *Computer Vision and Image Understanding*. 78 (2000) 138–156. <https://doi.org/10.1006/cviu.1999.0832>.
- [22] M. Weinmann, B. Jutzi, S. Hinz, C. Mallet, Semantic point cloud interpretation based on optimal neighborhoods, relevant features and efficient classifiers, *ISPRS Journal of Photogrammetry and Remote Sensing*. 105 (2015) 286–304. <https://doi.org/10.1016/j.isprsjprs.2015.01.016>.
- [23] M. Soilán, L. Truong-Hong, B. Riveiro, D. Laefer, Automatic extraction of road features in urban environments using dense ALS data, *International Journal of Applied Earth Observation and Geoinformation*. 64 (2018) 226–236. <https://doi.org/https://doi.org/10.1016/j.jag.2017.09.010>.
- [24] N. Izzati, H. Shamsudin, nurdiyana abdul razak, U. Yusof, mohd nor akmal Khalid, A Cellular Automata and Navigation Graph Framework in Simulating Crowd Behaviour at Bus Terminal Platform, 2015.
- [25] I. Puente, H. González-Jorge, J. Martínez-Sánchez, P. Arias, Review of mobile mapping and surveying technologies, *Measurement: Journal of the International Measurement Confederation*. 46 (2013) 2127–2145. <https://doi.org/10.1016/j.measurement.2013.03.006>.
- [26] V.T. Ngoc Nha, S. Djahel, J. Murphy, A Comparative Study of Vehicles’ Routing Algorithms for Route Planning in Smart Cities, *Vehicular Traffic Management for Smart Cities (VTM)*, First International Workshop on IEEE. (2012) 1–6. <https://doi.org/10.1109/VTM.2012.6398701>.